Int. J. Multiphase Flow Vol. 15, No. 6, pp. 997–1009, 1989
Printed in Great Britain.

0301-9322/89 $3.00 + 0.00

TURBULENT FORCED CONVECTIVE HEAT TRANSFER IN TWO-PHASE EVAPORATING DROPLET FLOW THROUGH A VERTICAL PIPE

T. F. LIN, J. F. JOU and C. H. HWANG
Department of Mechanical Engineering, National Chiao Tung University, Hsinchu, Taiwan, R.O.C.

(*Received* 1 *September* 1988; *in revised form* 29 *May* 1989)

Abstract—A physical model was developed to study heat transfer in turbulent dispersed flow at very high vapor quality in a vertical pipe by numerically solving the coupling governing differential equations for both phases. Major heat transfer mechanisms included in the model were the thermal nonequilibrium effects, droplet vaporization, droplet deposition on the duct wall and thermal radiative transfer. The predicted results indicated that vapor superheating is dominant for the cases with high wall superheat, otherwise droplet vaporization dominates the energy transport processes. Heat transfer during the droplet–wall interaction only exists at low wall superheat but in small amounts.

Key Words: dispersed flow heat transfer, turbulent forced convection

INTRODUCTION

Dispersed flow is characterized by the presence of a large quantity of fine liquid droplets in a continuous vapor flow. Momentum and heat transfer in this particular type of flow is largely affected by the droplet deposition on the duct wall, the vaporization of the droplets and the latent heat transport associated with it. The study of heat transfer in dispersed droplet flows is motivated by its importance in various applications, ranging from the operations of steam generators and cryogenic machinery, and the safety of nuclear reactors during the loss-of-flow accidents, to the spray combustion processes. Due to the complexities of the transport processes occurring in the flows, experimental approaches have failed to measure the detailed characteristics of the flows, and a rigorous computational physical model including all the major transport mechanisms has not yet been presented.

Models used to treat dispersed flow can be classified as empirical or phenomenological. Empirical models fit the experimental data to a proposed relationship, while phenomenological models take into account the physical processes involved. Phenomenological models can be further subdivided into models which utilize the existing heat transfer correlations and those that solve the conservation equations.

Correlations are normally developed using data from a limited number of sources and, as such, are typically limited to a range of flow conditions and one fluid. Many correlations begin with an accepted equation for single-phase heat transfer, such as the McAdams or Dittus–Boelter correlation, which is then modified to account for such effects as thermal nonequilibrium, droplet size, ratio of vapor to liquid velocities, void fraction etc.

Most phenomenological approaches start with an assumed heat transfer model which encompasses the major transfer processes occurring in the flow. Using correlations to characterize individual mechanisms, the model predicts the flow as it moves along the pipe. This requires a step-by-step solution scheme and must be implemented on a computer. The advantage in this approach is that it accounts for specific heat transfer mechanisms within the flow.

Various workers over the past two decades have attempted to explain the dispersed flow heat transfer through the identification of individual mechanisms. Thermodynamic nonequilibrium in dispersed two-phase flow was first suggested by Parker & Grosh (1961). Laverty & Rohsenow (1967), attempting to analyze the nonequilibrium effect in dispersed flow, proposed a model whereby heat transfer in the flow was considered to be a two-step process in which all the heat input from the wall is transferred to the vapor and then from the vapor to the liquid droplets.

Forslund & Rohsenow (1968) improved this model by accounting for droplet breakup and by modifying the drag coefficient of the accelerating drops. In addition, a "Leidenfrost" heat transfer from the wall to the droplets at low vapor qualities was included. Ganic & Rohsenow (1977) studied the structure of fully-developed dispersed flow, paying special attention to droplet deposition on the duct wall, the possible successive states of drop–wall interactions and the heat transfer to a single drop deposited on the heated wall. Bhatti (1977) assumed that the axial motion of droplets is with the local gas velocity without slip and investigated the transverse motion of droplets under the influence of Stokes' drag, buoyancy, gravity and inertia forces. Later, Ganic & Rohsenow (1979) examined the deposition of liquid drops in dispersed flow in greater detail. Chen *et al.* (1979) developed a phenomenological model and proposed a correlation of the convective vapor heat transfer in the post-CHF region by using a momentum-transfer analogy, allowing for thermodynamic nonequilibrium. Yao (1979) proposed a model to calculate the forced convection heat transfer in laminar droplet flow in the thermal entrance region of circular tubes with constant wall temperature, without considering the slip between the phases. The saturated droplets moving in the superheated vapor stream were treated as distributed heat sinks. The variations in the droplet size and population density of the droplets were not considered. Later, the reductions in droplet size, the increase in the vapor velocity and the dilution of the droplet density along the tube were all included by Rane & Yao (1980) and Yao & Rane (1980). Calculations were performed from the inlet of the thermal entrance region to the final fully-developed single-phase flow of vapor far downstream. Renksizbulut & Yuen (1983a, b) conducted experimental and numerical studies of droplet evaporation in a high-temperature gas flow past an evaporating liquid droplet and suggested correlations for drag and heat transfer coefficients. Rane & Yao (1981), Yao & Rane (1981) and Webb & Chen (1982) further considered the flow pattern as turbulent to determine the characteristics of dispersed flow. A much simpler prediction method was developed by Yoder & Rohsenow (1983) in predicting the steady-state dispersed flow heat transfer under constant heat flux conditions. Differential transport equations and accepted heat transfer correlations were employed to form a solution dependent only upon knowledge of the conditions at the dryout point. Thermal nonequilibrium is included in the analysis and the actual flow quality is determined from the local equilibrium conditions. Thermal radiation between the wall, vapor and droplets was demonstrated to be rather significant by Chung & Olafsson (1984) when the system is at high temperature. Despite these attempts to model heat transfer in dispersed flow, the detailed characteristics of momentum and heat transfer in dispersed flow are not well-understood. It was recently indicated by Varone & Rohsenow (1986), Koai *et al.* (1986) and Rohsenow (1988) that turbulence in the vapor is significantly modified by the presence of droplets and thus exhibits profound influences on the radial momentum and heat transfer in the dispersed flow, especially for low quality post-dryout heat transfer. To explain this turbulence modification by the droplets, a Nusselt number ratios R_{Nu} was proposed.

To elucidate the details of momentum and heat transfer, the dispersed flow model should be improved. In an attempt to investigtate the detailed heat transfer processes in dispersed flows, an improved physical model is developed for turbulent dispersed flow heat transfer in a vertical pipe. The governing partial differential equations, based on the continuum assumptions for both phases, representing the conservation of mass, momentum and energy for the vapor and droplet phases are solved numerically. To embody the couplings between the phases, the interfacial drag and convective heat transfer, the body force for each phase, the droplet evaporation and its effects on momentum and heat transfer in the flow are all taken into account. Numerical finite-difference procedures are employed to solve the governing equations with considerable attention being paid to the handling of the intimate couplings between the vapor and droplet phases. Computations are specifically performed for the mixture of fine liquid water droplets moving in their own vapor at high pressures normally encountered in the safety studies of nuclear reactors.

PHYSICAL AND MATHEMATICAL MODELS

Dispersed flow heat transfer consists of several individual heat transfer mechanisms as suggested in the literature review above. An accurate analysis of dispersed flow must include at least the major mechanisms. Thus, how the interactions among the drops, the vapor and the heated wall may affect

the wall heat transfer and the degree of thermodynamic nonequilibrium in the flow must be carefully modeled.

Despite the numerous attempts to model dispersed flow heat transfer, the predicted wall and vapor temperature variations are not in reasonable agreement with the experimental data, as reviewed by Varone & Rohsenow (1986). This indicates that our understanding of the heat transfer mechanisms occurring in the flow is still far from satisfactory. A better model which embodies more accurate physical mechanisms in the flow must be developed. As a preliminary attempt, the present study aims to develop a physical model which can improve our understanding of the flow and thermal characteristics in turbulent two-phase evaporating droplet flows.

Crowe (1978, 1979) presented a straightforward derivation based on conservation principles for both phases treated as continuums to yield a reliable set of continuity, momentum and energy equations for general, three-dimensional dispersed flows. Fundamental to the derivation of the two-fluid model for the dispersed flow presented in these papers is the transport theorem relating to the Lagrangian and Eulerian description of fluid motion with proper treatment of boundary effects at the phase interfaces. According to these conservation equations, terms considered to be important for the present problem are retained. In this fashion the governing equations for turbulent dispersed flows are obtained.

Before presenting the model equations, the physical situation under consideration is first described. A turbulent dispersed flow at the saturated temperature T_s enters the bottom end of a vertical pipe with a fully-developed velocity profile for both vapor and droplets. When the flow moves upwards in the pipe, the vapor gets superheated by receiving energy from the wall which is imposed by a constant heat flux q''_w in spite of losing some energy to evaporate the liquid droplets. The droplets are in fact at the saturated state. Since the vapor is at the thermal nonequilibrium state, the droplets evaporate with saturated vapor generated over their surfaces and the generated vapor gets heated as it moves into the vapor stream. For a water/steam system, the wall superheat can be relatively high and hence the thermal radiation heat transfer could be significant. Additionally, energy transfer resulting from droplet deposition on the pipe wall is significant at low wall superheat, as noted by Ganic & Rohsenow (1977, 1979) and Varone & Rohsenow (1986). These two processes are also included in the model.

For simplicity, at the tube inlet all the droplets are assumed to be the same size. In the flow droplets may move radially due to the presence of radial temperature and/or velocity gradients. A droplet will be pushed away from the wall due to its nonuniform evaporation near the wall. In reality, the droplet sizes are nonuniform both radially and axially. To simplify the analysis, in this study droplets are considered to be uniform in the radial direction r. Only axial variation in droplet size is accounted for.

In light of facilitating the analysis the following major simplifying assumptions are made:

(1) Steady axisymmetric flow and heat transfer is considered.
(2) Droplets are spherical and no droplet breakup occurs.
(3) The liquid is at the saturation state at the inlet point (dryout point) and remains so in the flow.
(4) The droplet size distribution can be characterized by an average drop size d and can only vary in the axial direction z.
(5) The vapor at the dryout point is at the saturated state.
(6) The axial heat conduction in the fluid is not included because low Péclet number flows are not considered.
(7) The effect of pipe wall heat conduction can be neglected.
(8) The vapor and droplet phases are treated as continuums in writing the transport equations.

With the above assumptions and boundary layer approximations, the governing equations for heat transfer in the flow can be described as follows:

(A) gas phase (continuous phase)

—continuity equation

$$\frac{\partial}{\partial z}(\varepsilon\rho_c u_c) + \frac{1}{r}\frac{\partial}{\partial r}(\varepsilon\rho_c r v_c) = \dot{m}_c, \qquad [1a]$$

—axial momentum equation

$$\varepsilon\rho_c\left(u_c\frac{\partial u_c}{\partial z}+v_c\frac{\partial u_c}{\partial r}\right)=-\varepsilon\frac{dp}{dz}+\frac{1}{r}\frac{\partial}{\partial r}\left[\varepsilon r(\mu_c+\mu_t)\frac{\partial u_c}{\partial r}\right]-f_{dz}-(u_c-u_d)\dot{m}_c-\varepsilon\rho_c g \quad [1b]$$

and

—energy equation

$$\varepsilon\rho_c c_{pc}\left(u_c\frac{\partial T_c}{\partial z}+v_c\frac{\partial T_c}{\partial r}\right)=\frac{1}{r}\frac{\partial}{\partial r}\left[\varepsilon r(k_c+k_t+k_r)\frac{\partial T_c}{\partial r}\right]-\dot{m}_c(i_c-i_s); \quad [1c]$$

and

(B) droplet phase (dispersed phase)

—continuity equation

$$\frac{\partial}{\partial z}[(1-\varepsilon)\rho_d u_d]+\frac{1}{r}\frac{\partial}{\partial r}[(1-\varepsilon)\rho_d r v_d]=-\dot{m}_c, \quad [1d]$$

—axial momentum equation

$$\rho_d(1-\varepsilon)\left(u_d\frac{\partial u_d}{\partial z}+v_d\frac{\partial u_d}{\partial r}\right)=f_{dz}-(1-\varepsilon)\rho_d g \quad [1e]$$

and

—energy equation

$$T_d=T_s=f(p). \quad [1f]$$

In the above equations u, v, T, i, p, ρ, μ and k, respectively, stand for the axial velocity, radial velocity, temperature, enthalpy, pressure, density, dynamic viscosity and thermal conductivity; g is the gravitational acceleration and ε is the vapor void fraction. The subscripts c and d denote the continuous (vapor) and dispersed (droplet) phases, respectively.

The first term on the r.h.s. of [1a] and [1d], $\dot{m}_c$, represents the volumetric vapor generation rate. If the chemical composition of the vapor and droplet are identical, mass transfer due to a concentration difference will not occur. Heat is transferred from the superheated vapor to the saturated droplets, and the subsequently generated vapor will be heated up to the local vapor stream temperature. As a result, the equivalent heat sink per unit volume is $n\pi d^2 h_{cd}\cdot(T_c-T_s)(1+B)$ and the associated volumetric vapor generation rate is $n\pi d^2 h_{cd}\cdot(T_c-T_s)/h_{LG}$. Here h_{cd} is the convection heat transfer coefficient from the superheated vapor to a saturated droplet, and n, d and h_{LG} are the droplet number density, average droplet diameter and latent heat of vaporization, respectively. The parameter B is the mass transfer number, a superheat parameter defined as $c_{pc}\cdot(T_c-T_s)/h_{LG}$. Here c_{pc} is the specific heat of the vapor. The heat transfer coefficient for the evaporation of water droplets in a superheated steam, as shown by Renksizbulut & Yuen (1983b), is

$$h_{cd}=\frac{k_c}{d}(2.0+7.4\,\mathrm{Re}_M^{0.5}\cdot\mathrm{Pr}_c^{0.33}); \quad [2]$$

where Re_M is the droplet Reynolds number based on the droplet size and its relative velocity to vapor,

$$\mathrm{Re}_M=\frac{\rho_c|u_c-u_d|d}{\mu_c}, \quad [3]$$

and Pr_c is the Prandtl number for the continuous phase.

The third term on the r.h.s. of [1b], also the first term on the r.h.s. of [1e], f_{dz}, stands for the aerodynamic force due to the velocity difference between the vapor and the droplets in the axial direction, and is defined as

$$f_{dz}=\frac{A_r C_{dz}\rho_c u_{rel}^2}{2}, \quad [4]$$

where A_r is the toal frontal area of the droplets. If droplets are treated as spheres, the frontal area of the droplets is $n\pi d^2/4$. In [4] u_{rel} is the relative axial velocity between the droplet and the vapor. With these relations substituted, [4] can be written as

$$f_{dz} = \frac{\text{sign}(u_c - u_d) n \frac{\pi d^2}{4} C_{dz} \rho_c (u_c - u_d)^2}{2}, \quad [5]$$

where $\text{sign}(u_c - u_d)$ has the following meaning:

$$\text{sign}(u_c - u_d) = \begin{cases} 1, & \text{if } u_c > u_d \\ -1, & \text{if } u_c < u_d \end{cases}. \quad [6]$$

Taking the evaporation on the droplet surfaces into account, the drag coefficient C_{dz}, in the droplet Reynolds number ranging from 10 to 260, was correlated by Renksizbulut & Yuen (1983b) as

$$C_{dz} = \frac{24}{\text{Re}_M} \frac{(1 + 0.2\,\text{Re}_M^{0.63})}{(1+B)^{0.2}} \quad [7]$$

For $\text{Re}_M < 10$, the following correlation proposed by White (1974) is used:

$$C_{dz} = \frac{24}{\text{Re}_M} + \frac{6}{1 + \text{Re}_M^{1/2}} + 0.4. \quad [8]$$

The fifth term on the r.h.s. of [1b] and the second term on the r.h.s. of [1e] represent the body forces. The fourth term on the r.h.s. of [1b], $(u_c - u_d)\dot{m}_c$, stands for the force due to evaporation of droplets, which is proportional to the velocity difference between the vapor and the droplets.

Turbulence in two-phase evaporating droplet flow is poorly understood. In vapor–droplet flow the turbulence is affected by complex interactions between the droplets and vapor, droplets and droplets, droplets and wall etc. Decent information on these interactions is currently unavailable, as indicated by Varone & Rohsenow (1986) and Zisselmar & Molerus (1979). In the present study the flow considered is at a high vapor void fraction and the two-phase effects on the turbulence are ignored. Therefore the results obtained in this study are not expected to be accurate for low-quality flow. Consequently, the single-phase correlation given by Cebeci & Bradshaw (1984) for eddy viscosity μ_t is used:

$$\mu_t = \rho_c \left\{ l \left[1 - \exp\left(-\frac{y}{A} \right) \right] \right\}^2 \cdot \left| \frac{\partial u_c}{\partial r} \right|, \quad [9]$$

here

$$A = 26 \left(\frac{\mu_c}{\rho_c} \right) \left(\frac{\tau_w}{\rho_w} \right)^{1/2} \quad [10]$$

and

$$l = R \cdot \left[0.14 - 0.08 \left(1 - \frac{y}{R} \right)^2 - 0.06 \left(1 - \frac{y}{R} \right)^4 \right], \quad [11]$$

where l is the mixing length, y is the distance from the pipe wall, τ_w is the wall shear stress and R is the pipe radius. The turbulent thermal conductivity k_t is evaluated through the concept of the turbulent Prandtl number Pr_t. The appropriate correlation for flow in a circular pipe is due to Malhotra & Kang (1984),

$$\text{Pr}_t = \frac{1}{(0.91 + 0.13\,\text{Pr}_c^{0.545})} \quad [12]$$

and

$$k_t = c_{pc} \cdot \frac{\mu_t}{\text{Pr}_t}. \quad [13]$$

Thermal radiation heat transfer in droplet flow is now described. At the high system pressure considered here vapor can be treated as an optically thick medium and a diffusion approximation is appropriate, as pointed out by Chung & Olafsson (1984) and Siegel & Howell (1981). Hence the

equivalent thermal conductivity due to thermal radiation k_r can be evaluated:

$$k_r = \frac{16\sigma_S}{3a_R} T_c^3, \qquad [14]$$

here a_R is the Rosseland absorption coefficient for vapor and is evaluated by the method developed by Abu-Romia & Tien (1967) and σ_S is the Stefan–Boltzmann constant. For the problem under consideration, radiative transfer from the wall to the droplets and from the vapor to the droplets was found to be relatively small compared to the corresponding convective mode.

Equations [1a–f] are subjected to the following boundary conditions:

$$\begin{aligned} &\text{at } z = 0, \quad u_c = u_d = u_e, \quad T_c = T_d = T_s; \\ &\text{at } r = 0, \quad \frac{\partial u_c}{\partial r} = \frac{\partial u_d}{\partial r} = \frac{\partial T_c}{\partial r} = 0; \\ &\text{at } r = R, \quad u_c = u_d = 0, \quad (k_c + k_r)\frac{\partial T_c}{\partial r} + q''_{wd} = q''_w. \end{aligned} \qquad [15]$$

Here u_e is the fully-developed turbulent velocity profile for single-phase flow at the entrance, which can be calculated by the procedures given by Kays & Crawford (1980).

Heat transfer resulting from droplet deposition on the pipe wall, q''_{wd}, is included in the model through the thermal boundary condition given in [15]. Empirically, from the studies of Ganic & Rohsenow (1977) and Varone & Rohsenow (1986), q''_{wd} can be expressed as

$$q''_{wd} = \epsilon \cdot v_0(1 - \varepsilon) \cdot \rho_d \cdot h_{LG}, \qquad [16]$$

here

$$v_0 = 0.17u^* \qquad [17]$$

and u^* is the friction velocity. An empirical correlation for calculating the heat transfer effectiveness ϵ during the droplet deposition process was proposed by Kendall & Rohsenow (1978).

It is noted in [15] that at the pipe wall the no-slip condition is applied to the droplet flow, i.e. $u_d = 0$. This is appropriate since the droplets are considered to be a continuum in the model.

The void fraction is defined as the ratio of the volume occupied by the vapor phase to the total volume at any cross section of the pipe. It is evaluated by the equation

$$\varepsilon = 1 - n\frac{\pi}{6}d^3. \qquad [18]$$

The droplet size is assumed to be radially uniform, as just mentioned, but can vary along the axial direction. By integrating the continuity equation for the droplet phase, [1d], over the pipe cross section and making use of [18], we obtain an equation for determining the axial variation of the droplet diameter:

$$\frac{d}{dz}\left(\rho_d \bar{u}_d n \frac{\pi}{6} d^3\right) \cdot \pi R^2 = -\int_0^R \dot{m}_c 2\pi r \, dr, \qquad [19]$$

here $\bar{u}_d$ is the average droplet velocity over the cross section considered. The average droplet diameter at the dryout point ($z = 0$) is estimated from the correlation proposed by Saha (1980):

$$\frac{d_e}{R} = 2.94\left\{\frac{G^2 x_e^2\left[\dfrac{\sigma}{g(\rho_d - \rho_c)}\right]^{1/2}}{\rho_c \cdot \sigma}\right\}^{-0.675}, \qquad [20]$$

here G is the mixture mass flux, x_e is the actual vapor quality at the entrance and σ is the surface tension.

Because it is assumed that no droplet breakup occurs, the total number of droplets passing through any pipe cross section per unit time is equal to the value at the tube inlet $n_e\bar{u}_e$,

$$n_e \bar{u}_e = n\bar{u}_d. \qquad [21]$$

Equations [1a–f], [18], [19] and [21] contain nine unknowns (u_c, u_d, v_c, v_d, T_c, p, ϵ, n and d), but we have only eight equations. Another equation must be sought. In analogy to single-phase pipe flows, the constraint to be satisfied in the analysis of a steady pipe flow is the overall mass balance for the vapor phase, which can be obtained by integrating [1a] with respect to r from 0 to R. In a dimensional form it is expressed as

$$\frac{\partial}{\partial z}\int_0^R \epsilon\rho_c r u_c \, dr = \int_0^R r\dot{m}_c \, dr. \qquad [22]$$

This equation is used in the solution process to check whether the pressure gradient, which is the first term on the r.h.s. of [1b], in the flow is correctly determined.

It is worth mentioning that the variations in the thermophysical properties of the steam with temperature and pressure are calculated from steam table data.

Some quantities of importance in illustrating heat transfer in dispersed flow are introduced here. The fraction of energy absorbed during the process of droplet evaporation (FR_{DE}), the fraction of energy absorbed during droplet deposition on the wall (FR_{DD}) and the fraction of energy causing the vapor to become superheated (FR_{VS}) due to convective and radiative heating are physically important in understanding the mechanisms of energy transport in the flow. By considering a differential control volume in the flow with differential pipe length dz, these fractions can be evaluated by the relations

$$FR_{DE} = \frac{1}{q''_w R}\int_0^R \dot{m}_c(i_c - i_s) r \, dr, \qquad [23]$$

$$FR_{DD} = \frac{q''_{wd}}{q''_w} \qquad [24]$$

and

$$FR_{VS} = 1 - FR_{DE} - FR_{DD}. \qquad [25]$$

The local two-phase Nusselt number along the duct is defined as

$$Nu = \frac{h_z(2R)}{k_c}, \qquad [26]$$

where the total local heat transfer coefficient is evaluated by

$$h_z = \frac{q''_w}{(T_w - T_b)}; \qquad [27]$$

here T_w and T_b are, respectively, the wall temperature and the bulk temperature of the vapor.

SOLUTION METHODOLOGY

The finite-difference approximations to the partial derivatives are used to discretize the governing differential equations [1a–e]. The centered difference is used for the radial diffusion terms, while in the axial direction we use the upwind difference because the flow is convection-dominant. Nonuniform step sizes are employed in both the radial and axial directions. 121 grid points are placed in the radial direction from the centerline to the pipe wall. The step sizes in the axial direction range from 0.1 to $2R$ with the gridlines more concentrated in the inlet region.

Since equations [1a–e] are nonlinear, linearization is necessary. This was implemented by iteratively solving the finite-difference equations which were put in the form of tridiagonal matrix equations and solved by the Thomas algorithm, described by Anderson *et al.* (1984).

The solution procedures are briefly outlined as follows:

(1) For any axial location, guess a dp/dz and solve the finite-difference form of equation [1b] for the distribution of u_c.
(2) Integrate the vapor continuity equation [1a] numerically to find the vapor radial velocity v_c.
(3) Solve the finite difference form of [1c] to find the temperature profile T_c.

(4) Solve the finite difference form of [1e] to find the distribution of droplet axial velocity u_d.
(5) Integrate [1d] to get the profile of droplet radial velocity v_d.
(6) Substitute the droplet axial velocity u_d into [19] and [21] to find the droplet number density n and droplet size d. Use the results for n and d to get the void fraction ε from [18].
(7) Check the satisfaction of the overall conservation of mass, [22] and the convergence of the velocity and temperature fields in each iteration. If yes, repeat the above procedures for the next axial location. If no, guess a new dp/dz and repeat procedures (1)–(6) for the current axial location. The tolerance for the satisfaction of the overall mass conservation equation and the convergence criterion of the velocity and temperature fields are set to be 10^{-5} and 10^{-3}, respectively.

Since the dispersed flow treated here is at high vapor void fraction, the heat transfer mechanism in it is close to that in the single-phase flow of vapor. The solution technique used here to solve the conservation equations is a natural extension of that employed for single-phase heat transfer problems by adding the continuity and momentum equations for the droplet flow to the computation. For the purpose of verifying our numerical scheme, the predicted wall superheats are compared with the data of Bennett *et al.* (1967) in figure 1 for dispersed flow in a vertical pipe of diameter $D = 0.012$ m. Good agreement is noted in figure 1. Additionally, the predicted wall superheats for the cases shown in figure 1, predicted using a finer grid system of doubling the number of nodes in both the axial and radial directions, differ from that predicted by the original grid by $<3\%$. Through these program tests, the proposed numerical scheme is considered to be suitable for solving the problem investigated.

RESULTS AND DISCUSSION

Over the past two decades a number of experimental studies have been performed to investigate dispersed flow heat transfer. In these studies, data are mainly provided for the distributions of wall superheat, $(T_w - T_s)$. Information on the detailed thermal and hydrodynamic characteristics is not currently available. To validate the proposed physical model, the predicted axial distributions of wall superheat are compared with the data of Bennett *et al.* (1967) and Era *et al.* (1966) in figures 1 and 2 for three cases representing the results for high, medium and low wall superheats. For the high wall superheat case excellent agreement is noted. The agreements gradually become worse for the lower wall superheat cases. In particular, for the low wall superheat case (figure 2) the agreement is not good. This disagreement with the data of Era *et al.* is due to the low-quality

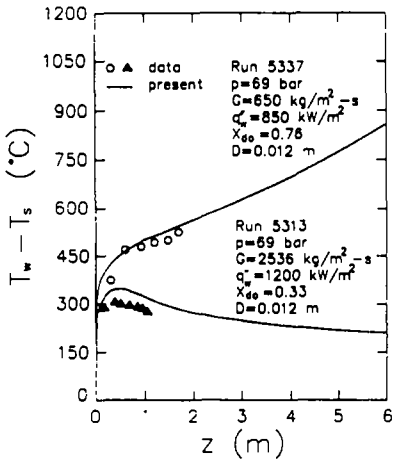

Figure 1. Comparison of the predicted wall superheat with the data of Bennett *et al.* (1967).

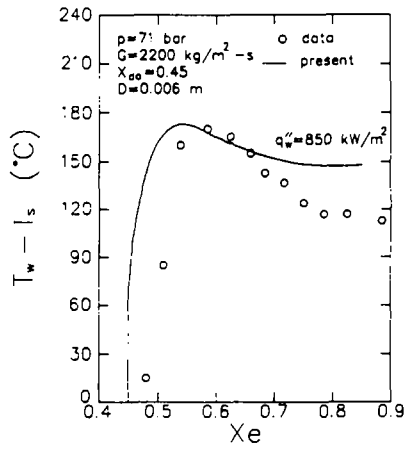

Figure 2. Comparison of the predicted wall superheat with the data of the Era *et al.* (1966).

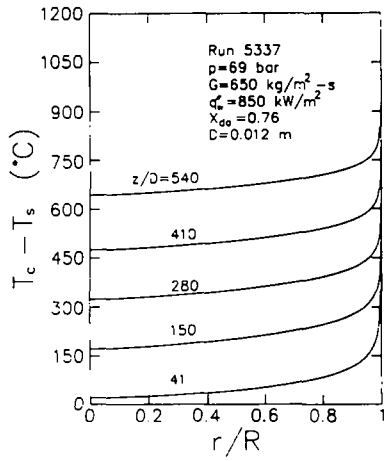

Figure 3. The vapor temperature profiles at various axial locations for the high wall superheat case.

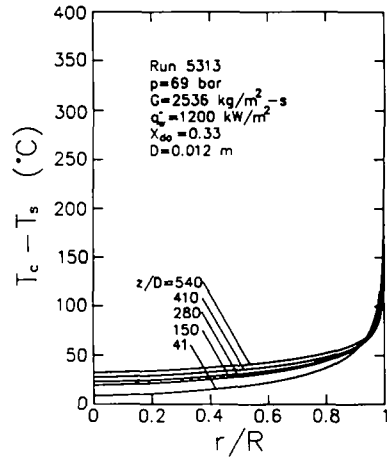

Figure 4. The vapor temperature profiles at various axial locations for the medium wall superheat case.

dryout ($x_{do} = 0.45$) in this case. A very large amount of droplets in the flow greatly changes the turbulence in the vapor, as noted by Varone & Rohsenow (1986) and Koai *et al.* (1986). The single-phase eddy viscosity employed here is simply inappropriate in this case. Therefore, the model is considered to be suitable for providing qualitative results for understanding the heat transfer characteristics in the dispersed flow at low liquid content. In what follows we present these characteristics.

Presented in figures 3 and 4 are the radial distributions of the vapor superheat, $(T_c - T_s)$, at various axial locations for the high and medium wall superheat cases. Significant vapor superheating is observed in figure 3 for the high $\Delta T_w (= T_w - T_s)$ case, indicating that a substantial amount of heat input to the flow through the pipe wall goes to the vapor through convective and radiative transfer processes. The vapor is thus in a highly nonequilibrium state. This is simply because the liquid content in the flow is small for the dryout vapor quality at 0.76. For the medium ΔT_w case ($x_{do} = 0.33$) the vapor superheating shown in figure 4 is only very slight. The result is a direct consequence of the dominant heat transfer in the flow by the droplet evaporation when the liquid content is high. These trends in the vapor superheat can be distinctly seen by examining the bulk vapor temperature variations given in figure 5. It is of interest to note that at low vapor quality ($x_{do} = 0.33$) the vapor superheat quickly levels off after the flow leaves the dryout point and stays at this level as the flow moves downstream.

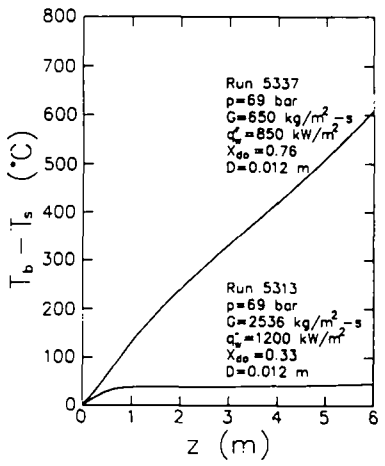

Figure 5. The distributions of the bulk vapor temperature.

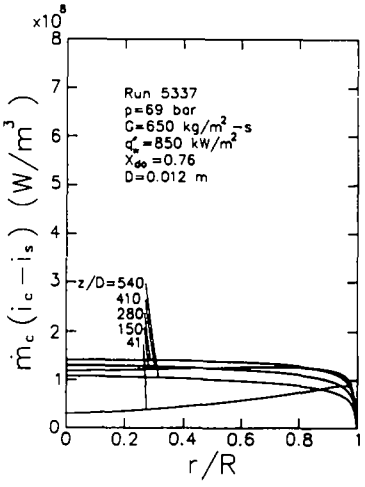

Figure 6. The distribution of the heat sink due to droplet vaporization for the high wall superheat case.

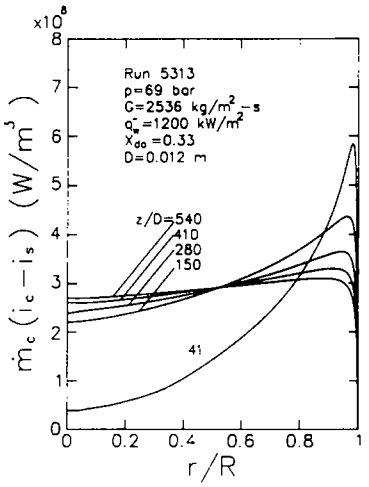

Figure 7. The distribution of the heat sink due to droplet vaporization for the medium wall superheat case.

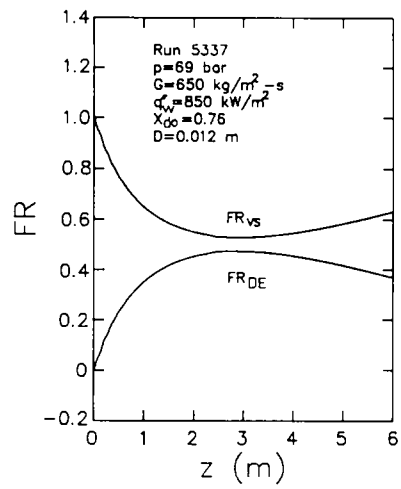

Figure 8. The predicted fractions of energy for various heat transfer processes for the high wall superheat case.

Energy absorption by droplet evaporation has been considered to be important in dispersed flow heat transfer in many studies (Yao & Rane 1980; Webb & Chen 1982). Figures 6 and 7 show this energy absorption predicted for the present study for the high and medium ΔT_w cases. At high x_{do} (figure 6) the heat sink due to droplet evaporation is not large because only a small amount of droplets is present in the flow. When the droplets present in the flow are in large quantities at low x_{do}, the energy absorbed by droplet evaporation is rather significant (figure 7). In addition, the heat sink for the low x_{do} case is found to be more pronounced in the near-wall regions, especially in the entry portion of the pipe.

To unravel the detailed heat transfer characteristics, a close examination of the various heat transfer mechanisms in the flow is required. In the physical model presented in this study three heat transfer mechanisms are taken into consideration. They are: (1) heat transfer from the wall to the single-phase vapor by convective and radiative transfer processes; (2) heat transfer from the superheated vapor to the liquid droplets causing droplet vaporization; and (3) heat transfer from the wall to the droplets during the droplet–wall interactions. According to these three mechanisms, the energy transferred to the dispersed flow from the uniform heating imposed on the pipe wall can be conveniently divided into three portions: the fraction FR_{VS}, defined in [25], contributes to heating up the vapor from the saturated condition to the superheated state; the fraction FR_{DE}, defined in [23], causes droplet evaporation and brings the saturated vapor generated on the droplet

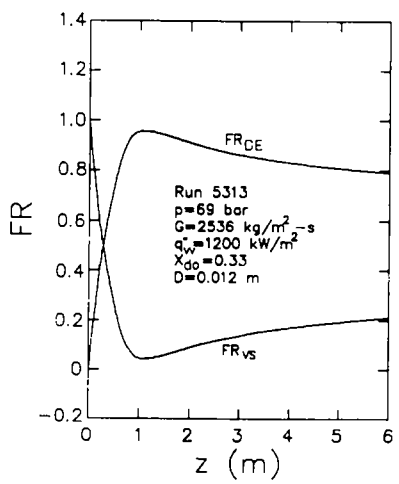

Figure 9. The predicted fractions of energy for various heat transfer processes for the medium wall superheat case.

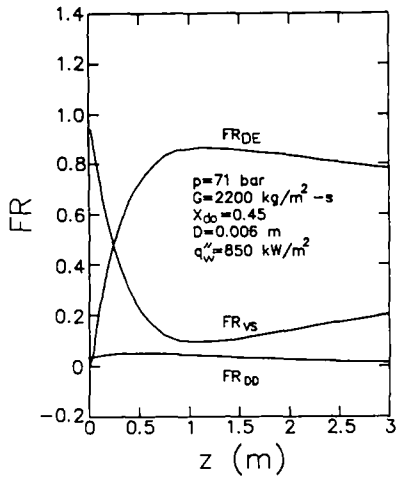

Figure 10. The predicted fractions of energy for various heat transfer processes for the low wall superheat case.

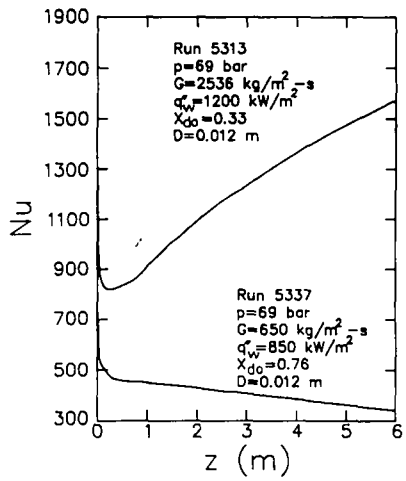

Figure 11. The local two-phase Nu distributions.

surfaces to the local superheated vapor temperature; and the third fraction FR_{DD}, defined in [24], accounts for the energy absorbed during the droplet deposition on the wall.

The distributions of FR_{VS}, FR_{DE} and FR_{DD} for the three different wall superheat cases are illustrated in figures 8–10. At high wall superheat (figure 8), the wall temperature is above the Leidenfrost temperature and no droplet deposition on the wall occurs. Accordingly, $FR_{DD} = 0$. The result in figure 8 clearly indicates that in the entry portion of the pipe the heat input to the flow mostly goes to the vapor and thus causes it to become superheated. As the vapor becomes superheated, it transfers energy to the droplets by the convective process, resulting in droplet evaporation. More and more energy goes to the vaporizing droplets when the degree of vapor superheating increases. Consequently, FR_{VS} decreases but FR_{DE} increases as the flow moves downstream. In the downstream region ($z > 3$ m), although the vapor superheat increases, the energy absorption by droplet evaporation gradually reduces—a result of the dilution of the droplets by the flow acceleration, [21], and the reduction in droplet size through the vaporization of droplets. It is worth noting that in this region $FR_{VS} > FR_{DE}$.

For the medium wall superheat case the result in figure 9 also indicates that $FR_{DD} = 0$, since T_w still exceeds the Leidenfrost point. In the presence of a large quantity of liquid droplets in the flow ($x_{do} = 0.33$) FR_{VS} decreases and FR_{DE} increases drastically in the flow direction, and droplet vaporization absorbs about 80% of the heat input to the flow except in the region near the dryout location. When the wall superheat is low, the droplet deposition on the wall accounts for about 4% of the energy transport in the flow, as seen in figure 10. The variations of FR_{VS} and FR_{DE} in this case are similar to those for the medium wall superheat case.

Finally, we present the local two-phase Nu in the flow. At high wall superheat the Nu shown in figure 11 decreases monotonically in the flow direction, as does that encountered in forced convection single-phase flows through pipes. This is due to the low liquid content in the flow ($x_{do} = 0.76$) and the heat transfer characteristics in it being close to those in single-phase flows. For the case with a high liquid content ($x_{do} = 0.33$) Nu drops quickly in the entry portion of the pipe but after a certain location it rises steadily. This result implies that the presence of a large quantity of droplets exhibits pronounced effects on the heat transfer in the flow, and Nu is much larger—a similar result to those found by Chung & Olafsson (1984).

CONCLUDING REMARKS

A physical model embodying the thermal nonequilibrium effects, droplet deposition on the duct wall, droplet evaporation and thermal radiative transfer has been developed for heat transfer in turbulent dispersed flow. The model is expected to yield accurate results at very high vapor quality. The predicted results for the cases considered indicate that vapor superheating is important for high

vapor quality dispersed flow and that the vaporization of droplets becomes dominant when the liquid content is high. Heat transfer during the droplet–wall interaction process only exists for the low wall superheat case but in a small amount.

In developing the model several important processes were ignored, namely, the droplet–droplet interaction, droplet breakup, turbulence modification by the presence of droplets etc. These processes are particularly important in low vapor quality flows, as measured by Era *et al.* (1966). Therefore appropriate models for these processes are required.

Acknowledgements—The financial support of this study, partly by the Institute of Nuclear Energy Research and partly by National Science Council of Taiwan, R.O.C., is greatly appreciated.

REFERENCES

ABU-ROMIA, M. M. & TIEN, C. L. 1967 Appropriate mean absorption coefficients for infrared radiation of gases. *ASME Jl Heat Transfer* **89,** 321–327.

ANDERSON, D. A., TANNEHILL, J. C. & PLETCHER, R. H. 1984 *Computational Fluid Mechanics and Heat Transfer*, pp. 125–129. Hemisphere, Washington, D.C.

BENNETT, A. W., HEWITT, G. F., KEARSEY, H. A. & KEEYS, R. K. F. 1967 Heat transfer to steam water mixtures flowing in uniformly heated tubes in which the critical heat flux has been exceeded. Report AERE-R 5373.

BHATTI, M. S. 1977 Dynamics of a vaporizing droplet in laminar entry region of a straight channel. *ASME Jl Heat Transfer* **99,** 574–579.

CEBECI, T. & BRADSHAW, P. 1984 *Physical and Computational Aspects of Convective Heat Transfer*, pp. 216–220. Springer, New York.

CHEN, J. C., OZKAYNAK, F. T. & SUNDARAM, R. K. 1979 Vapor heat transfer in post-CHF region including the effect of thermodynamic nonequilibrium. *Nucl. Engng Des.* **51,** 143–155.

CHUNG, J. N. & OLAFSSON, S. I. 1984 Two-phase droplet flow convection and radiative transfer. *Int. J. Heat Mass Transfer* **27,** 901–910.

CROWE, C. T. 1978 Heat transfer in dispersed-phase flow. In *Proc. 6th Int. Heat Transfer Conf.* pp. 463–469.

CROWE, C. T. 1979 On the dispersed phase flow equations. In *Symposium in Chemical Process, and Energy Engineering Systems (Proc. ICHMT Semin. 1978)*, Vol. 2, pp. 23–32. Hemisphere, Washington, D.C.

ERA, A., GASPARI, G. P., HASSID, A., MILANI, A. & ZAVATTARELLI, R. 1966 Heat transfer data in liquid deficient regions for steam–water mixtures at 70 kg/cm flowing in tubular and annular conduits. Report CISE R-184.

FORSLUND, R. P. & ROHSENOW, W. M. 1968 Dispersed flow film boiling. *ASME Jl Heat Transfer* **90,** 399–407.

GANIC, E. N. & ROHSENOW, W. M. 1977 Dispersed flow heat transfer. *Int. J. Heat Mass Transfer* **20,** 855–866.

GANIC, E. N. & ROHSENOW, W. M. 1979 On the mechanism of liquid drop deposition in two-phase dispersed flow. *ASME Jl Heat Transfer* **101,** 288–294.

KAYS, W. M. & CRAWFORD, M. E. 1980 *Convective Heat and Mass Transfer*, 2nd edn, pp. 196–203. McGraw-Hill, New York.

KENDALL, G. E. & ROHSENOW, W. M. 1978 Heat transfer to impacting drops and post critical heat flux dispersed flow. MIT Heat Transfer Lab. Report No. 85694-100.

KOAI, K. K., VARONE, A. F. & ROHSENOW, W. M. 1986 Comparison of post dryout heat transfer prediction methods. Paper presented at the *U.S.–Japan Joint Heat Transfer Symp.*, Lake Placid, N.Y.

LAVERTY, W. F. & ROHSENOW, W. M. 1967 Film boiling of saturated nitrogen flowing in a vertical tube. *ASME Jl Heat Transfer* **89,** 90–98.

MALHOTRA, A. & KANG, S. S. 1984 Turbulent Prandtl number in circular pipes. *Int. J. Heat Mass Transfer* **27,** 2158–2161.

PARKER, J. D. & GROSH, R. J. 1961 Heat transfer to a mist flow. AEC R&D Report ANL-6291.

RANE, A. G. & YAO, S. C. 1980 Heat transfer of evaporating droplet flow in low pressure systems. *Can. J. chem. Engng* **58,** 303–308.

RANE, A. G. & YAO, S. C. 1981 Convective heat transfer to turbulent droplet flow in circular tubes. *ASME Jl Heat Transfer* **103,** 679–684.

RENKSIZBULUT, M. & YUEN, M. C. 1983a Experimental study of droplet evaporation in a high-temperature air stream. *ASME Jl Heat Transfer* **105,** 384–388.

RENKSIZBULUT, M. & YUEN, M. C. 1983b Numerical study of droplet evaporation in a high-temperature air stream. *ASME Jl Heat Transfer* **105,** 389–397.

ROHSENOW, W. M. 1988 Post dryout heat transfer prediction method. *Int. Commun. Heat Mass Transfer* **15,** 559–569.

SAHA, P. 1980 A nonequilibrium heat transfer model for a dispersed droplet post-dryout regime. *Int. J. Heat Mass Transfer* **23,** 483–492.

SIEGEL, R. & HOWELL, J. R. 1981 *Thermal Radiation Heat Transfer*, 2nd edn, pp. 497–516. Hemisphere, Washington, D.C.

VARONE, A. F. JR & ROHSENOW, W. M. 1986 Post dryout heat transfer prediction. *Nucl. Engng Des.* **95,** 315–327.

WEBB, S. W. & CHEN, J. C. 1982 A numerical model for turbulent nonequilibrium dispersed flow heat transfer. *Int. J. Heat Mass Transfer* **25,** 325–335.

WHITE, F. M. 1974 *Viscous Fluid Flow*, pp. 200–215. McGraw-Hill, New York.

YAO, S. C. 1979 Convective heat transfer of laminar droplet flow in thermal entrance region of circular tubes. *ASME Jl Heat Transfer* **101,** 480–483.

YAO, S. C. & RANE, A. G. 1980 Heat transfer of laminar mist flow in tubes. *ASME Jl Heat Transfer* **102,** 678–683.

YAO, S. C. & RANE, A. G. 1981 Numerical study of turbulent droplet flow heat transfer. *Int. J. Heat Mass Transfer* **24,** 785–793.

YODER, G. L. JR & ROHSENOW, W. M. 1983 A solution for dispersed flow heat transfer using equilibrium fluid conditions. *ASME Jl Heat Transfer* **105,** 10–17.

ZISSELMAR, R. & MOLERUS, O. 1979 Investigation of solid–liquid pipe flow with regard to turbulence modification. In *Two-phase Momentum, Heat, and Mass Transfer in Chemical Process, and Energy Engineering Systems*, pp. 145–157. Hemisphere, Washington, D.C.